PNAS RESEARCH ARTICLE | NEUROSCIENCE

Dopamine D2 receptors in hilar mossy cells regulate excitatory transmission and hippocampal function

Michelle C. Gulfo[a], Joseph J. Lebowitz[b], Czarina Ramos[a], Dong-Woo Hwang[c], Kaoutsar Nasrallah[a,1,2], and Pablo E. Castillo[a,d,1]

Edited by Julie Kauer, Stanford University, Stanford, CA; received May 4, 2023; accepted October 30, 2023 by Editorial Board Member Huda Akil

Hilar mossy cells (MCs) are principal excitatory neurons of the dentate gyrus (DG) that play critical roles in hippocampal function and have been implicated in brain disorders such as anxiety and epilepsy. However, the mechanisms by which MCs contribute to DG function and disease are poorly understood. A defining feature of MCs is the promoter activity of the dopamine D2 receptor (D2R) gene (*Drd2*), and previous work indicates a key role for dopaminergic signaling in the DG. Additionally, the involvement of D2R signaling in cognition and neuropsychiatric conditions is well known. Surprisingly, though, the function of MC D2Rs remains largely unexplored. In this study, we show that selective and conditional removal of *Drd2* from MCs of adult mice impaired spatial memory, promoted anxiety-like behavior, and was proconvulsant. To determine the subcellular expression of D2Rs in MCs, we used a D2R knockin mouse which revealed that D2Rs are enriched in the inner molecular layer of the DG, where MCs establish synaptic contacts with granule cells (GCs). D2R activation by exogenous and endogenous dopamine reduced MC to dentate GC synaptic transmission, most likely by a presynaptic mechanism. In contrast, exogenous dopamine had no significant impact on MC excitatory inputs and passive and active properties. Our findings support that MC D2Rs are essential for proper DG function by reducing MC excitatory drive onto GCs. Lastly, impairment of MC D2R signaling could promote anxiety and epilepsy, therefore highlighting a potential therapeutic target.

hippocampus | mossy cell | dentate gyrus | dopamine | memory

Significance

Growing evidence indicates that hilar mossy cells (MCs) of the dentate gyrus play critical but incompletely understood roles in memory and brain disorders, including anxiety and epilepsy. Dopamine D2 receptors (D2Rs), implicated in cognition and several psychiatric and neurological disorders, are considered to be characteristically expressed by MCs. Still, the subcellular localization and function of MC D2Rs are largely unknown. We report that removing the *Drd2* gene specifically from MCs of adult mice impaired spatial memory and was anxiogenic and proconvulsant. We also found that D2Rs were enriched where MCs synaptically contact dentate granule cells (GC) and reduce MC-GC transmission. This work uncovered the functional significance of MC D2Rs, thus highlighting their therapeutic potential in D2R- and MC-associated pathologies.

The human and rodent hippocampus is well recognized for its roles in spatial learning and memory (1–3). As the main input region to the hippocampus proper that discriminates between sensory inputs, the dentate gyrus (DG) is critical for these functions (1, 2). Hilar mossy cells (MCs) of the DG are crucial yet poorly understood players in hippocampal function (4), including spatial learning and novelty detection, as well as disease processes, such as mood disorders and epilepsy (5–12). MCs have unique anatomical properties that position them to powerfully shape the function of the DG. In addition to mediating local disynaptic inhibition onto dentate granule cells (GCs)—i.e., MC-inhibitory interneuron-GC—, each MC sends direct excitatory projections to as many as 35,000 GCs along as much as 75% of the hippocampal axis (13). In turn, GCs provide both monosynaptic excitation and disynaptic inhibition to MCs (14). While MC properties and functions are being elucidated, the molecular mechanisms underlying MC involvement in critical physiological and pathophysiological processes remain largely unknown.

One hallmark of MCs is the promoter activity of the dopamine D2 receptor gene (*Drd2*). Remarkably, MCs are the only excitatory hippocampal neurons that exhibit promoter activity of the *Drd2* gene in mice (15, 16). Dopamine D2 receptors (D2Rs), along with D3 and D4 receptors, make up the D2-like family of dopamine receptors and are $G_{i/o}$-coupled. Dopamine D1 and D5 receptors comprise the D1-like family of dopamine receptors and are G_s-coupled. D2Rs have been extensively studied throughout the brain for their roles in cognition, mood disorders, schizophrenia, and Parkinson's disease (17). Quantitative autoradiography for D2Rs in human tissue revealed a marked absence of signal in the GC layer (GCL) and a strong band of signal in the input layers to the GCs (18). In cats, this signal is particularly robust in the inner molecular layer (IML), which mainly contains MC axons targeting GCs (18). Promoter activity of the *Drd2* gene is a feature of MCs widely used to selectively target them (11, 12, 19–21). One study has tested the role of D2R signaling in MC excitability ex vivo (22), but the functional significance of MC D2Rs in vivo is unknown. Hippocampal dopaminergic signaling has been implicated in processes now associated with MCs, such as spatial memory, novelty detection, anxiety-like behavior, and epilepsy (23–30). In addition, dopamine release in the hippocampus and DG from ventral tegmental area and locus coeruleus fibers (24, 31, 32) suggests that MC D2Rs could be activated in vivo. Additionally, *Drd2* gene expression is a signature feature of MCs that could be conserved in humans, as supported by D2R

Author contributions: M.C.G., J.J.L., K.N., and P.E.C. designed research; M.C.G., J.J.L., C.R., D.-W.H., and K.N. performed research; M.C.G., J.J.L., C.R., D.-W.H., and K.N. analyzed data; and M.C.G., J.J.L., K.N., and P.E.C. wrote the paper.

The authors declare no competing interest.

This article is a PNAS Direct Submission. J.K. is a guest editor invited by the Editorial Board.

[1]To whom correspondence may be addressed. Email: kaoutsar.n@gmail.com or pablo.castillo@einsteinmed.edu.

[2]Present address: Department of Biological Sciences, Fordham University, Bronx, NY 10458.

This article contains supporting information online at https://www.pnas.org/lookup/suppl/doi:10.1073/pnas.2307509120/-/DCSupplemental.

Published December 8, 2023.

autoradiography (18). Therefore, determining the role of MC D2Rs is critical to understanding hippocampal function in health and disease.

To investigate the role of MC D2Rs, we genetically and selectively removed the *Drd2* gene from MCs in adult mice and assessed the resulting behavioral and cellular phenotypes. We found that this manipulation induced a deficit in spatial memory and promoted anxiety-like behavior, two key modalities regulated by the hippocampus and MCs. In addition, *Drd2* removal from MCs increased the severity of and susceptibility to experimentally induced seizures, although it did not significantly impact MC excitatory inputs and MC active and passive properties. Using a tagged D2R knockin mouse, we revealed that D2Rs are highly expressed in the IML and, consistent with this finding, D2R activation reduced MC-GC synaptic transmission in a presynaptic manner. Thus, our results indicate that MC D2Rs modulate DG functions at least in part by reducing MC-GC transmission.

Results

Efficient and Selective Removal of the *Drd2* Gene from Hilar MCs. To determine the role of MC D2Rs, we selectively removed the *Drd2* gene from MCs. To this end, we bilaterally injected a Cre-expressing virus under the CaMKII promoter (AAV5-CaMKII-mCherry-Cre, or AAV5-CaMKII-mCherry as a control) in the dorsal and ventral hilus of 3- to 3.5-mo-old floxed *Drd2* (*Drd2*$^{fl/fl}$) mice (Fig. 1*A*). As MCs are the only excitatory neurons of the hippocampus that show activity of the *Drd2* promoter (15, 16), and viral gene expression is under the excitatory *CaMKII* promoter (33), Cre was expected to induce significant loss of

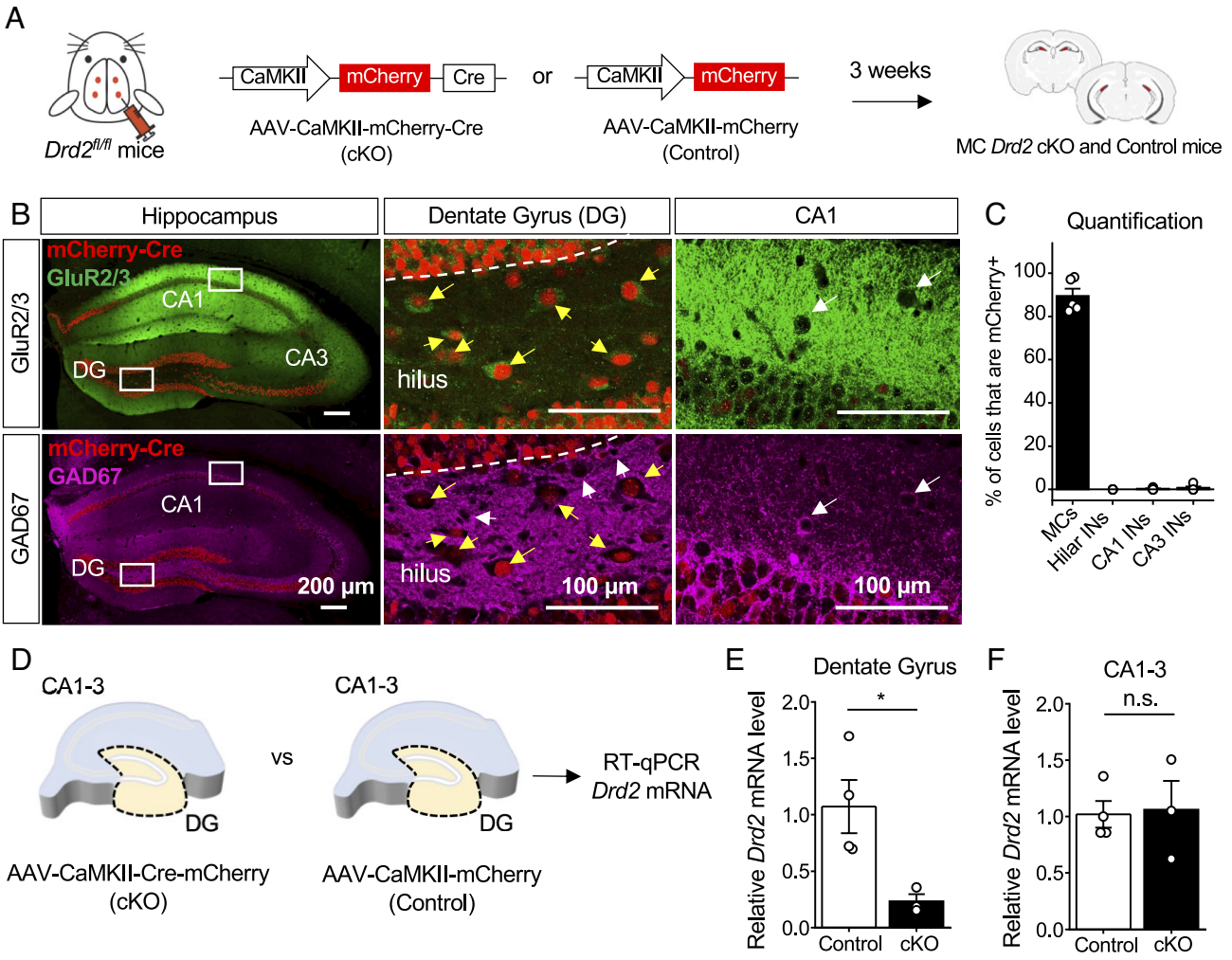

Fig. 1. Efficient and selective removal of *Drd2* from hilar MCs. (*A*) Schematic diagram illustrating the experimental strategy to conditionally and selectively KO the *Drd2* gene from MCs in adult mice. AAV5-CaMKII-mCherry-Cre (cKO) or AAV5-CaMKII-mCherry (Control) virus was injected bilaterally into the ventral and dorsal DG of *Drd2*$^{fl/fl}$ mice (4 total injection sites) to generate MC *Drd2* cKO or Control mice, respectively. All experiments on these mice were performed at least 3 wk after viral injections. (*B* and *C*) Confocal images (*B*) and quantification (*C*) revealing high viral expression (mCherry) in hilar MCs (89.4 ± 3.4% of MCs are mCherry positive, N = 5 mice) and a lack of infection in hippocampal INs (0% of hilar INs, 0.3 ± 0.2% of CA1 INs and 0.7 ± 0.6% of CA3 INs are mCherry positive, N = 5 mice). (*B*) *Left*, low-magnification images of the hippocampus of a coronal section immunostained for GluR2/3 and GAD67 and assessed for viral efficiency (% of MCs infected) and specificity (% of INs infected). Note that viral expression (mCherry signal) is present throughout the hilus. *Middle, Inset* images of the hilus showing that mCherry-expressing hilar neurons (red) are MCs (yellow arrows) identified as GluR2/3-positive (green, *Top*) and GAD67-negative neurons (magenta, *Bottom*). Note the absence of mCherry expression in hilar INs (white arrows, *Middle Bottom*). *Right, Inset* images of CA1 showing examples of mCherry-negative CA1 INs identified as GluR2/3-negative and GAD67-positive (magenta, white arrows). (*D–F*) RT-qPCR analysis. Levels of *Drd2* mRNA relative to *β-actin* mRNA were quantified in the DG and CA1-3 subfields of *Drd2*$^{fl/fl}$ mice injected with AAV5-CaMKII-mCherry (Control) vs. AAV5-CaMKII-mCherry-Cre (cKO) viruses. (*D*) Schematic showing that DG and CA1-3 sections were dissected from hippocampi of both MC *Drd2* cKO and Control mice for RT-qPCR analysis. (*E* and *F*) Levels of *Drd2* mRNA relative to *β-actin* mRNA in the DG (*E*) or CA1-3 region (*F*) for each animal are reported as a fold-difference from that of the Control animals' mean using the $2^{-\Delta\Delta Ct}$ method (*SI Appendix*). Relative *Drd2* mRNA was significantly reduced in the DG (Control: 1.1 ± 0.2, N = 4; cKO: 0.2 ± 0.1, N = 3; control vs. cKO: $P = 0.03$, unpaired *t* test) but not in CA1-3 areas (control: 1.0 ± 0.1, N = 4; cKO: 1.1 ± 0.3, N = 3; control vs. cKO: $P = 0.88$, unpaired *t* test) of cKO mice as compared to Control mice. Data are represented as mean ± SEM. *$P < 0.05$, n.s. > 0.5.

Drd2 expression only in MCs. After 3 wk were allowed for viral expression, the injection strategy yielded MC *Drd2* conditional knockout (cKO) and Control mice (Fig. 1*A*), and we confirmed this by validating the efficiency, selectivity, and functionality of the viruses. Because of the well-recognized differences in dopamine dynamics and receptor levels between sexes and across the estrous cycle (34, 35), we used male mice as a first approach to test for the functional significance of MC D2Rs.

To test for viral efficiency and selectivity, we performed double immunohistochemistry on injected hippocampal slices for GluR2/3 and GAD67, commonly used in the mouse hilus as markers for MCs and interneurons (INs), respectively (5, 15) (Fig. 1*B*). Quantification of MCs infected with Cre (mCherry positive) confirmed that the virus infected MCs with high efficiency (~90%) (Fig. 1*C*). Next, we assessed viral selectivity for excitatory neurons to ensure that D2R-expressing INs of CA1-3 (15, 16) were not targeted by Cre. Comparison of the cell types infected with Cre virus (mCherry positive) confirmed that the virus injected in the hilus and driven by the *CaMKII* promoter was indeed selective for excitatory neurons and did not appreciably infect INs of the hilus or CA1 and CA3 regions (Fig. 1*C*). Although mCherry-Cre was expressed in GCs, these excitatory neurons do not display promoter activity of the *Drd2* gene (15, 16). We then tested the effectiveness and selectivity of the Cre virus by performing RT-qPCR on injected hippocampal slices for *Drd2* mRNA relative to *β-actin* mRNA. We dissected the DG from the CA regions in hippocampal slices from each animal to separately analyze the two *Drd2*-expressing cell populations of the hippocampus—i.e., MCs of the DG and INs of the CA regions (Fig. 1*D*). We found that the level of *Drd2* mRNA was significantly reduced in the DG of MC *Drd2* cKO animals as compared to Control animals (Fig. 1*E*). In contrast, there was no difference in *Drd2* mRNA level in the CA regions between Control and cKO animals (Fig. 1*F*). These RT-qPCR assessments strongly support that the Cre virus effectively reduced the level of *Drd2* mRNA from Control levels only in MCs of the DG, and not in INs of the CA regions. Having validated our experimental approach, we assessed the behavioral impact of genetic *Drd2* removal from MCs.

Deleting the *Drd2* Gene from Hilar MCs Impaired Object Location Memory (OLM) but Not Object Recognition Memory (ORM). Hippocampal dopaminergic signaling has been implicated in various forms of spatial memory (23, 24, 29). Therefore, we assessed the role of MC D2R signaling in spatial memory by testing MC *Drd2* cKO and Control mice in the OLM task. This well-recognized test has been used to study MC function (5, 8, 36). In our experiment, MC *Drd2* cKO and Control mice were allowed to freely explore two identical objects in the training configuration for 4 min. One hour later, one object was moved, and mice were allowed to freely explore the two objects in the testing configuration for 5 min (Fig. 2*A*). Mice that displayed a preference for the moved object during testing [moved object preference score >55%; moved object preference score = (moved object exploration time/total object exploration time)*100] were considered to pass the test and have intact spatial memory. Mice with a marked preference (>60%) for either object during training and mice with a total exploration under 3 s in training or testing were excluded (8, 36). As expected, we found that in training there

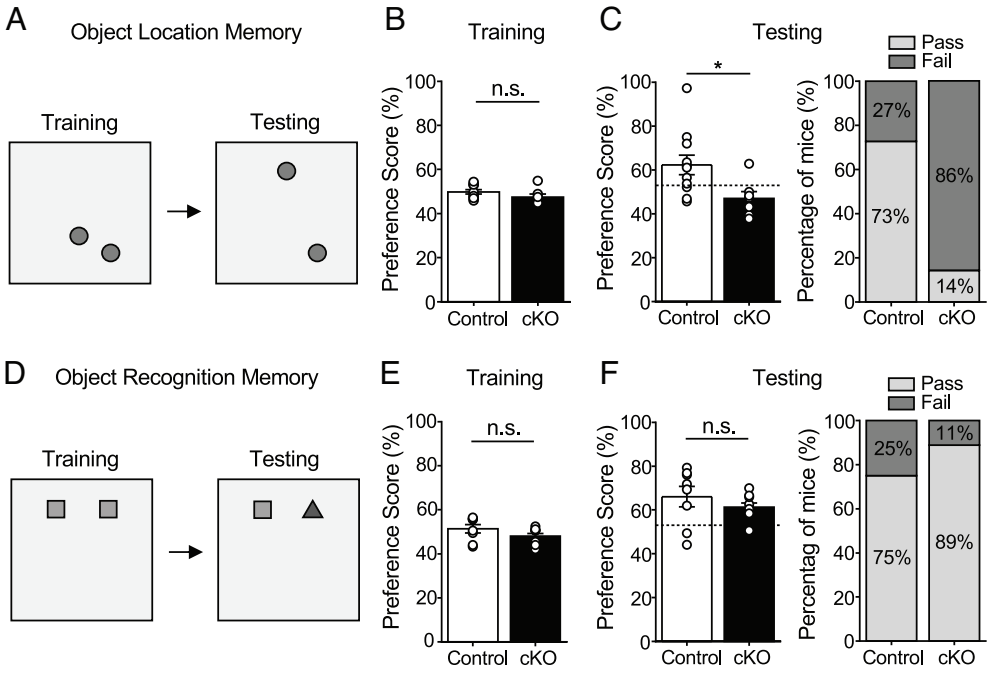

Fig. 2. Deleting *Drd2* from hilar MCs impaired OLM but not ORM. (*A–C*) OLM test. (*A*) OLM test schematic (Training duration: 4 min; Testing duration: 5 min; Interval between training and testing: 1 h). (*B*) Control and MC *Drd2* cKO mice did not show any significant difference in preference score during training (Control: 49.8 ± 0.9%, N = 11; cKO: 47.5 ± 1.4%, N = 7; Control vs. cKO: $P = 0.2$, unpaired *t* test). (*C*) MC *Drd2* cKO mice showed impaired OLM (mean moved object preference score < 55%) with significant reduction in preference for the moved object during testing, as compared to Control mice (Control: 62. 4 ± 4.5%, N = 11; cKO: 47.0 ± 3.1%, N = 7; Control vs. cKO: $P = 0.025$, unpaired *t* test). The dashed horizontal line indicates the threshold to pass the OLM test, corresponding to a mean preference score > 53%. *Right*, percentage of mice that passed the OLM test. The pass rate was significantly greater in Control than cKO mice (Control: 73%, cKO: 14%; $P = 0.025$, Fisher's exact test). (*D–F*) ORM test. (*D*) ORM test schematic (Training duration: 4 min; Testing duration: 5 min; Interval between training and testing: 1 h). (*E*) MC *Drd2* cKO and Control mice did not show significant difference in preference score during training (Control: 51.4 ± 1.9%, N = 8; cKO: 48.0 ± 1.3%, N = 9; Control vs. cKO, $P = 0.16$, unpaired *t* test). (*F*) MC *Drd2* cKO and Control mice both showed no impairment in ORM (mean preference score > 55%) and no difference in performance (Control: 66.1 ± 4.6%, N = 8; cKO: 61.3 ± 1.9%, N = 9; Control vs. cKO: $P = 0.37$, unpaired *t* test). The dashed horizontal line indicates the threshold to pass the ORM test, corresponding to a mean preference score > 53%. *Right*, the pass rate was not greater in Control as compared to cKO mice ($P = 0.9176$, right-sided Fisher's exact test). Data are represented as mean ± SEM. *$P < 0.05$, n.s. > 0.1.

was no difference in preference for the would-be-moved object between MC *Drd2* cKO and Control mice (Fig. 2*B*). In testing, the performance of cKOs was impaired compared to Controls, as measured by analysis of preference scores (Fig. 2 *C*, *Left*) and pass rate (Fig. 2 *C*, *Right*). There was no difference in total object exploration time between Control and cKO animals in training or testing (*SI Appendix*, Fig. S1*A*). Finally, to test whether expressing Cre alone could contribute to the observed OLM impairment (Fig. 2*C*), we injected the Cre-expressing virus in wild-type mice (AAV5-CaMKII-mCherry-Cre, or AAV5-CaMKII-mCherry as a control; *SI Appendix*, Fig. S3*A*). Cre had no significant effect on OLM (*SI Appendix*, Fig. S3 *A* and *B*). In all, these results support that the MC D2Rs are essential in spatial memory.

The role of the hippocampus in recognition memory is more nuanced than its role in spatial memory (37), as other cortical brain regions contribute to this type of memory (36). The DG and MCs have been implicated by several studies in novelty detection and recognition memory (8, 38, 39), although one study reported that inhibiting MC activity has no impact on ORM (5). Nonetheless, novel events trigger dopamine release in the hippocampus (23, 24), and particularly hippocampal dopamine D1/D5 receptor signaling has been linked to enhancing ORM (30) and enhancing spatial memory following novelty exposure (23, 24). To directly address the potential role of MC D2Rs in recognition memory, we tested MC *Drd2* cKO and Control mice in the ORM task, which has been used in studies of MC function (5, 8, 36). We used the same scoring scheme and inclusion criteria as for OLM, except that in testing, one object was replaced instead of being moved (Fig. 2*D*). In training, we found no difference in preference for the would-be-replaced object between MC *Drd2* cKO and Control mice (Fig. 2*E*). In testing, there was no difference in performance between the two groups of mice as measured by either preference score (Fig. 2 *F*, *Left*), and the pass rate was not greater in Control as compared to cKO mice (Fig. 2 *F*, *Right*). Finally, to probe maximally for a deficit in ORM in MC *Drd2* cKO mice, we challenged the animals to an interval of 24 h between training and testing. Still, both groups of mice passed the test, and there was no difference in performance between the two groups (*SI Appendix*, Fig. S1*B*). Our results indicate that MC D2R signaling is not critical for ORM. The results also support that deleting the *Drd2* from MCs does not affect sensory processing and cognition but selectively interferes with spatial memory.

Deleting *Drd2* from Hilar MCs Promotes Anxiety-Like Behavior. MCs have been implicated in controlling anxiety-like behavior (1, 3, 8–10). The hippocampus can detect conflict and choices to be made between approach and avoidance in the environment, and this detection likely underlies both its roles in spatial memory and anxiety-like behavior (1). To test whether MC *Drd2* cKO mice exhibited alterations in anxiety-like behavior, we first ran them in the Open Field Test (OFT), which assesses locomotor and anxiety-like behaviors (Fig. 3*A*). We found that MC *Drd2* cKO mice spent more time at the edges and avoided the center of the arena as compared to Control mice (Fig. 3*B*), suggesting an increase in anxiety-like behavior (40). The cKO mice also traveled a significantly shorter total distance (*SI Appendix*, Fig. S2*A*) in the center of the Open Field. The reduced time MC *Drd2* cKO mice spent in the center of the arena could not be explained by changes in motor ability including total tracklength and average velocity (Fig. 3*C* and *SI Appendix*, Fig. S2*A*). These results suggest that deleting the *Drd2* gene from MCs promotes anxiety-like behavior. To test this possibility directly, we used the Elevated Plus Maze (EPM) (41). MC *Drd2* cKO and Control mice were allowed to freely explore the EPM for 10 min (Fig. 3*D*). We found that MC *Drd2* cKO mice spent significantly

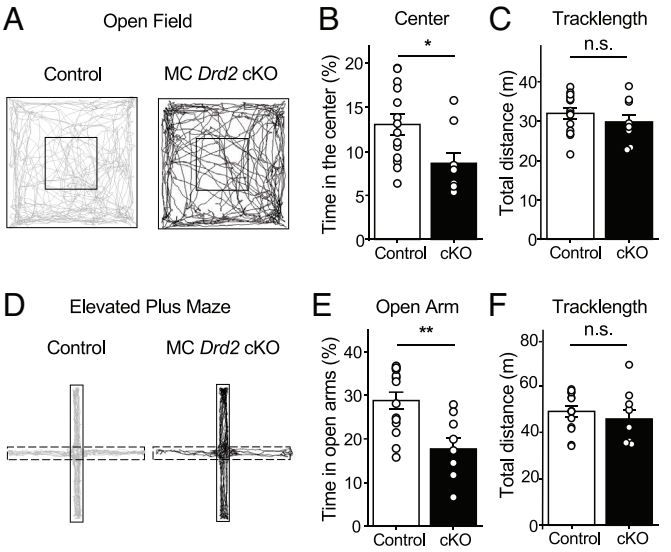

Fig. 3. Deleting *Drd2* from MCs promoted anxiety-like behavior. (*A*–*C*) OFT. (*A*) Representative track maps of a Control (*Left*, gray trace) and an MC *Drd2* cKO mouse (*Right*, black trace) in the open field. (*B*) MC *Drd2* cKO mice spent a significantly lower percentage of the test time in the center (inner square) of the open field as compared to Control animals (Control: 13.1 ± 1.2%, N = 14; cKO: 8.7 ± 1.2%, N = 9, Control vs. cKO: $P = 0.014$, Mann–Whitney *U* test). (*C*) No significant difference in total tracklength was observed between Control and cKO animals (Control: 32.0 ± 1.3%, N = 14; cKO: 29.8 ± 1.8%, N = 9; Control vs. cKO: $P = 0.34$, unpaired *t* test). Data are from minutes 0 to 6 of the test. (*D*–*F*) EPM. (*D*) Representative track maps of a Control (*Left*, gray trace) and an MC *Drd2* cKO mouse (*Right*, black trace) in the EPM. Dashed lines correspond to the open arm. (*E*) MC *Drd2* cKO mice spent a significantly lower percentage of test time in the open arms of the EPM than Controls (Control: 28.8 ± 2.0%, N = 14; cKO: 17.7 ± 2.4%, N = 9, Control vs. cKO: $P = 0.0019$, unpaired *t* test). No significant difference in total tracklength was observed between Control and cKO animals (Control: 49.0 ± 2.2 m, N = 14; cKO: 45.8 ± 3.9 m, N = 9, Control vs. cKO: $P = 0.45$, unpaired *t* test). Data are from minutes 0 to 10 of the test. Data are represented as mean ± SEM. n.s. $P > 0.2$, $^*P < 0.05$, $^{**}P < 0.01$.

less time (Fig. 3*E*) and traveled a significantly shorter total distance (*SI Appendix*, Fig. S2*B*) in the open arms of the maze as compared to Control mice. This anxiety-like phenotype in MC *Drd2* cKO mice could not be explained by motor deficits, as there was no difference in total distance traveled by (Fig. 3*F*) or average velocity of (*SI Appendix*, Fig. S2*B*) Control and cKO mice. In addition, expressing Cre alone in wild-type mice had no effect on the OFT and the EPM test (*SI Appendix*, Fig. S3 *C* and *D*). Altogether, these results indicate that MC D2Rs may have an anxiolytic function.

Deleting the *Drd2* Gene from Hilar MCs Increases Seizure Severity and Susceptibility. In addition to anxiety-like behavior, MCs play a key role in temporal lobe epilepsy (4, 5, 11, 12). There is also evidence that dopamine regulates seizures from the limbic system (27). Germline deletion of *Drd2* is proconvulsive and excitotoxic, particularly in the CA3 area (26, 28). Pharmacologic studies also support an antiepileptic role of D2R signaling in the hippocampus (27). Therefore, we examined the contribution of MC D2Rs in regulating seizure activity using the well-established kainic acid model of acute seizure induction (42) (Fig. 4*A*). MC *Drd2* cKO and Control mice were injected with kainic acid (20 mg/kg, i.p.) and their seizure stage was scored every 10 min for 2 h according to the modified Racine scale (*SI Appendix*). MC *Drd2* cKO mice had a higher cumulative Racine score than Control mice across the scoring period, with an approximately twofold difference present by the end of it (Fig. 4*B*). Thus, over the 2-h scoring period, MC *Drd2* cKO mice had significantly more severe seizures than Control mice (Fig. 4 *B* and *C*). The cKOs also had a greater susceptibility to seizures, as they reached the convulsive seizure stage significantly sooner than Controls did (Fig. 4*D*). Of

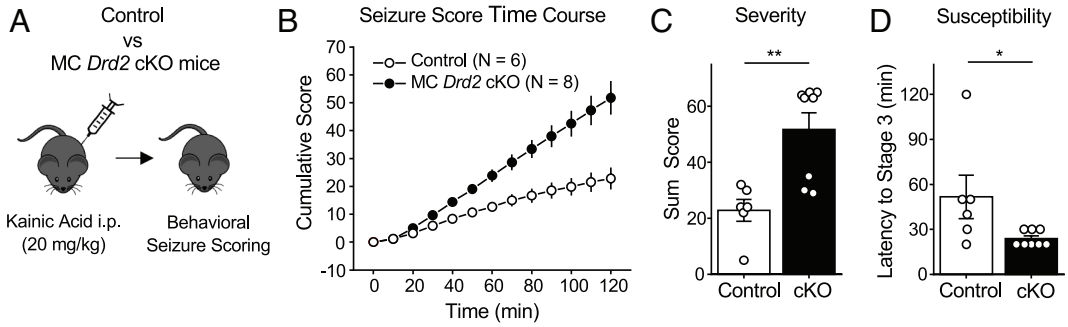

Fig. 4. Deleting the *Drd2* gene from MCs increased KA-induced seizure severity and susceptibility. (*A*) Experimental timeline. Seizures were acutely induced using a single KA i.p. injection (20 mg/kg) and scored using a modified Racine scale for 120 min. (*B–D*) The cumulative Racine score at the end of 120 min of scoring (*B*) was significantly greater in MC *Drd2* cKO mice than Control mice (*C*, severity; Control: 22.8 ± 3.9%, N = 6; cKO: 51.8 ± 6.0%, N = 8; Control vs. cKO: $P = 0.0095$, Mann–Whitney *U* test). MC *Drd2* cKO mice also showed a significant decrease in latency to convulsive seizures as compared to Control mice (*D*, susceptibility; Control: 51.7 ± 14.5%, N = 6; cKO: 23.8 ± 1.8%, N = 8; Control vs. cKO: $P = 0.025$, Mann–Whitney *U* test). Data are presented as mean ± SEM. $*P < 0.05$; $**P < 0.01$.

note, expression of Cre alone in wild-type mice had no significant effect on KA-induced seizures (*SI Appendix*, Fig. S*3 E–H*). These results support that MC D2R signaling can act as a powerful negative regulator of seizure activity.

D2Rs Are Enriched in the IML of the Dentate Gyrus. Having uncovered a role for MC D2Rs in vivo, we sought to determine potential cellular and molecular mechanisms underlying the phenotypes we observed. We began by investigating the subcellular distribution of D2Rs in MCs. Given the low specificity and sensitivity of D2R antibodies for addressing such question in tissue (17), we used a knockin mouse with a superecliptic pHluorin (SEP) epitope fused to the N terminus of endogenous D2Rs (43, 44). Live labeling of SEP-D2Rs was achieved by incubating ex vivo coronal slices containing the DG with an α-GFP antibody prior to permeabilization. At low power, SEP-D2R signal appeared as a distinct band surrounding the GCL as visualized with DAPI, corresponding to the IML (Fig. 5*A*). This IML signal was not present when the coronal slice was not incubated with the α-GFP antibody (Fig. 5*B*). When imaged at 63X using AiryScan, SEP-D2R signal bounding the GCL appeared as puncta (Fig. 5*C*), similar to the punctate distribution of D2Rs previously observed in the midbrain (43, 44). Intensity analysis of SEP-D2R signal confirmed the clear enrichment of D2Rs in the IML relative to that measured in the GCL and MML (Fig. 5*D*). The lack of promoter activity of the *Drd2* gene in GCs (15, 16) strongly suggests that the IML signal arises from MC axons. Notably, no SEP-D2R puncta were observed on the MC cell bodies in the hilus which were identified by GluR2/3 labeling (Fig. 5*E*). We next examined whether SEP-D2Rs were selectively expressed on MC axon terminals by comparing the colocalization of surface SEP-D2R puncta with either the vesicular glutamate transporter 1 (VGlut1) or the vesicular GABA transporter (VGAT) (Fig. 5 *F* and *G*). As would be predicted for SEP-D2R expression on MC axon terminals, the degree of colocalization between SEP-D2R and VGlut1 was significantly greater than that between SEP-D2R and VGAT (Fig. 5*F*). SEP-D2R and VGAT signals were not colocalized, confirming the predicted expression in the IML of knockin animals (Fig. 5 *F* and *G*). The enrichment of D2Rs in the IML with no apparent surface receptors on the somatodendritic compartment of MCs supports the hypothesis that D2R acts to decrease transmitter release from MC axon terminals.

D2R Activation Depresses MC–GC Excitatory Transmission by a Presynaptic Mechanism. Our results thus far supported that MC D2Rs, likely expressed in MC axon terminals, are critical to hippocampal function in vivo. We therefore hypothesized that a potential mechanism by which MC D2R signaling mediates its effects on behavior is by modulating MC-GC synaptic transmission, which we tested using hippocampal slice electrophysiology. We performed whole-cell voltage-clamp recordings of GCs and elicited MC-GC excitatory postsynaptic currents (EPSCs) by electrically stimulating MC axons in the IML with inhibitory synaptic transmission blocked—i.e., in the presence of the $GABA_A$ receptor antagonist picrotoxin (100 μM) and the $GABA_B$ receptor antagonist CGP55845 (3 μM). We found that bath application of dopamine (20 μM, 15 min) significantly and reversibly depressed MC-GC EPSCs (Fig. 6 *A* and *B*). This depression was blocked in the presence of the competitive D2-like antagonist sulpiride (1 μM) (Fig. 6 *A* and *B*). In addition, it was accompanied by an increase in paired-pulse ratio (PPR) (Fig. 6*C*), consistent with a presynaptic mechanism. D2R antagonism had no effect on baseline transmission (Fig. 6*D*), suggesting that MC D2Rs are not tonically active at the MC-GC synapse. The dopamine-mediated depression of MC-GC synaptic transmission was not accompanied by changes in GC holding current or input resistance (Fig. 6*E*), also consistent with a presynaptic mechanism. MC *Drd2* removal precluded the dopamine-mediated depression of MC-GC transmission (Fig. 6*F*) and PPR increase (Fig. 6*G*), supporting that dopamine depresses MC-GC transmission by targeting presynaptic D2Rs. Deleting *Drd2* from MCs had no significant effect on basal neurotransmitter release, as indicated by the lack of PPR change (Fig. 6*G*), further supporting the absence of tonic activity of MC D2Rs on MC-GC transmission. Lastly, we examined whether endogenous dopamine could also modulate MC-GC synaptic transmission. To test this possibility, we use amphetamine, which potently releases dopamine from dopaminergic terminals (45). Bath application of D-amphetamine hemisulphate (20 μM) also induced a reversible reduction of MC-GC transmission that was abolished in the continuous presence of sulpiride (1 μM) (Fig. 6*H*). Together, these findings indicate that activation of MC D2R by exogenous and endogenous dopamine reversibly reduced MC-GC transmission, most likely by inhibiting glutamate release from MC axon terminals.

Although a presynaptic mechanism of dopamine-mediated depression of MC-GC transmission is consistent with the D2R enrichment in the IML where MCs synaptically contact GCs (Fig. 5), D2R expression in other MC compartments and synaptic inputs cannot be discarded, especially given the low sensitivity of the SEP-D2R KI approach. However, we found that dopamine application had no significant effect on MC active and passive properties (e.g., threshold current, number of action potentials per injected

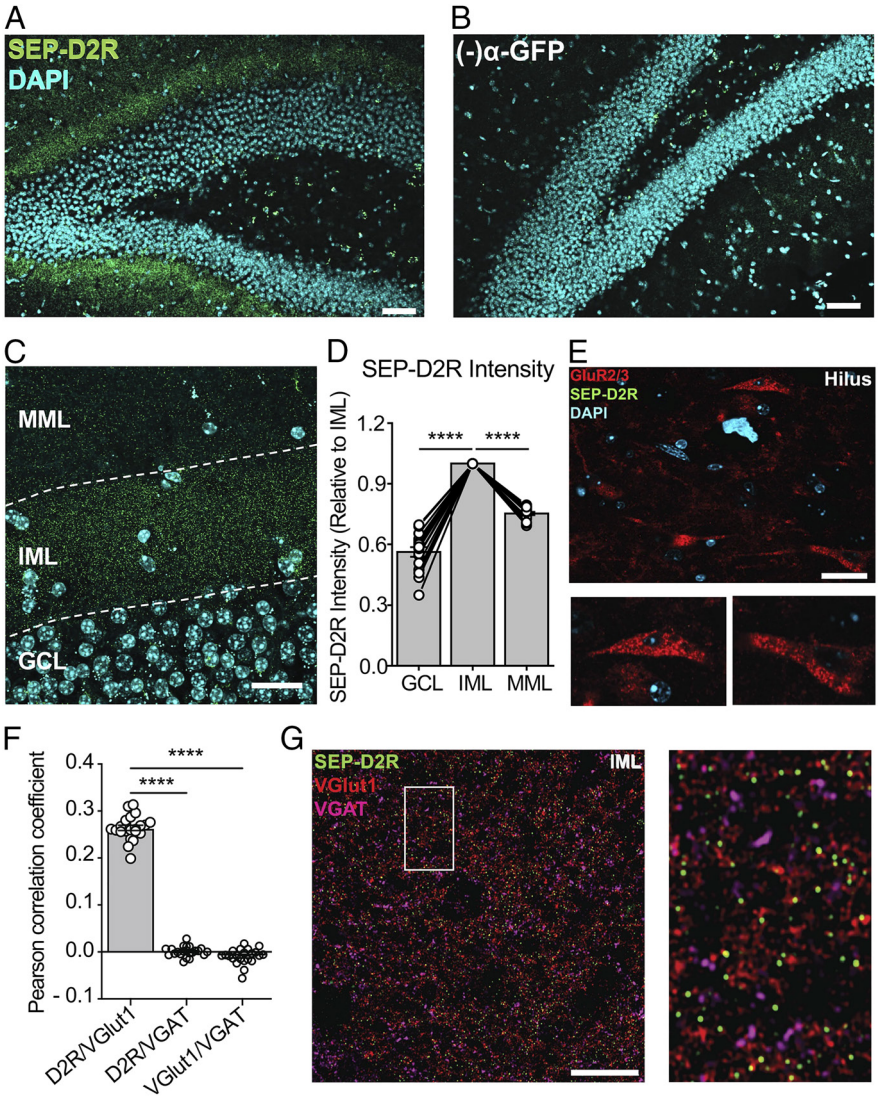

Fig. 5. Enriched D2R expression in the IML of the dentate gyrus. (*A*) 20X image of D2R labeling in the DG in a SEP-D2R knockin mouse following signal amplification with an α-GFP antibody conjugated to Alex Fluor 488. The SEP epitope was live-labeled prior to permeabilization to selectively visualize surface D2Rs. (Scale bar: 100 μm.) (*B*) 20X image of the DG in an SEP-D2R mouse that was not incubated with the α-GFP antibody. Imaging and visualization parameters are identical to those used in *A*. (Scale bar: 100 μm.) (*C*) Maximum intensity projection of a z-stack (thickness = 2.94 μm) taken at 63X of SEP-D2R labeling in the IML. SEP-D2R labeling is abundant in the IML where MC terminals reside with less apparent labeling in the GCL and MML. (Scale bar: 20 μm.) (*D*) Intensity quantification of SEP-D2R signal in the GCL and MML normalized to that measured in the IML imaged in single z-planes (IML vs. GCL: $P < 0.0001$; IML vs. MML: $P < 0.0001$; n = 16 images/4 slices/4 animals; Dunnett's multiple comparison test following repeated-measures one-way ANOVA). (*E*) 63X image of GluR2/3 labeling in the hilus following antibody-amplification of SEP-D2R. Surface SEP-D2R puncta are absent from GluR2/3 containing cell bodies (*Insets*). (*F*) Pearson correlation coefficients between surface SEP-D2Rs, VGlut1, and VGAT measured in single plane images of the IML (D2R/VGlut1 vs. D2R/VGAT: $P < 0.0001$; D2R/VGlut1 vs. VGlut1/VGAT: $P < 0.0001$; D2R/VGAT vs. VGlut1/VGAT: $P = 0.1722$; n = 22 images/5 slices/2 animals; Tukey's multiple comparison test following one-way ANOVA). (*G*) Representative AiryScan image of surface SEP-D2R labeling in the IML colabeled for VGlut1 (red) and VGAT (magenta). Zoomed *Inset* highlights the frequent colocalization of surface SEP-D2R puncta with VGlut1 (+) but not VGAT (+) terminals. (Scale bar: 10 μm.) Data are represented as mean ± SEM. ****$P < 0.0001$.

current step, and input resistance—see *Material and Methods*) monitored under pharmacological blockade of excitatory and inhibitory synaptic transmission (*SI Appendix*, Fig. S4 *A–E*). In addition, dopamine did not affect spontaneous EPSC amplitude and frequency in MCs (*SI Appendix*, Fig. S4 *F* and *G*) or evoked GC-MC EPSCs (*SI Appendix*, Fig. S4*H*). Thus, these results support our anatomical and functional findings (Figs. 5 and 6), indicating that MC D2Rs may primarily modulate MC and DG functions by reducing glutamate release from MC projections to GCs.

Discussion

This study reveals a role of MC D2R signaling in crucial aspects of hippocampus-dependent cognitive function and diseases. By selectively and conditionally removing D2Rs from MCs in adult mice, we demonstrate that MC D2Rs are essential for spatial memory and play anxiolytic and anticonvulsant roles. At the cellular level, dopamine negatively controlled MC-GC synaptic transmission via MC D2R activation, while it did not significantly impact MC excitability or excitatory inputs. Furthermore, we show anatomical evidence for D2R enrichment in MC axons. In light of the extensive and powerful connections that MCs make to GCs, it follows that MCs strongly regulate DG function. Given the diffuse nature of dopamine release and extensive dopaminergic projections within the hippocampus, dopaminergic signaling via presynaptic D2Rs emerges as an ideally suited neuromodulatory mechanism for controlling MC-GC excitatory transmission and hippocampal function. Our study provides mechanistic insights into MC and D2R function in memory, anxiety-like behaviors, and seizures, suggesting MC D2Rs as a potential therapeutic target.

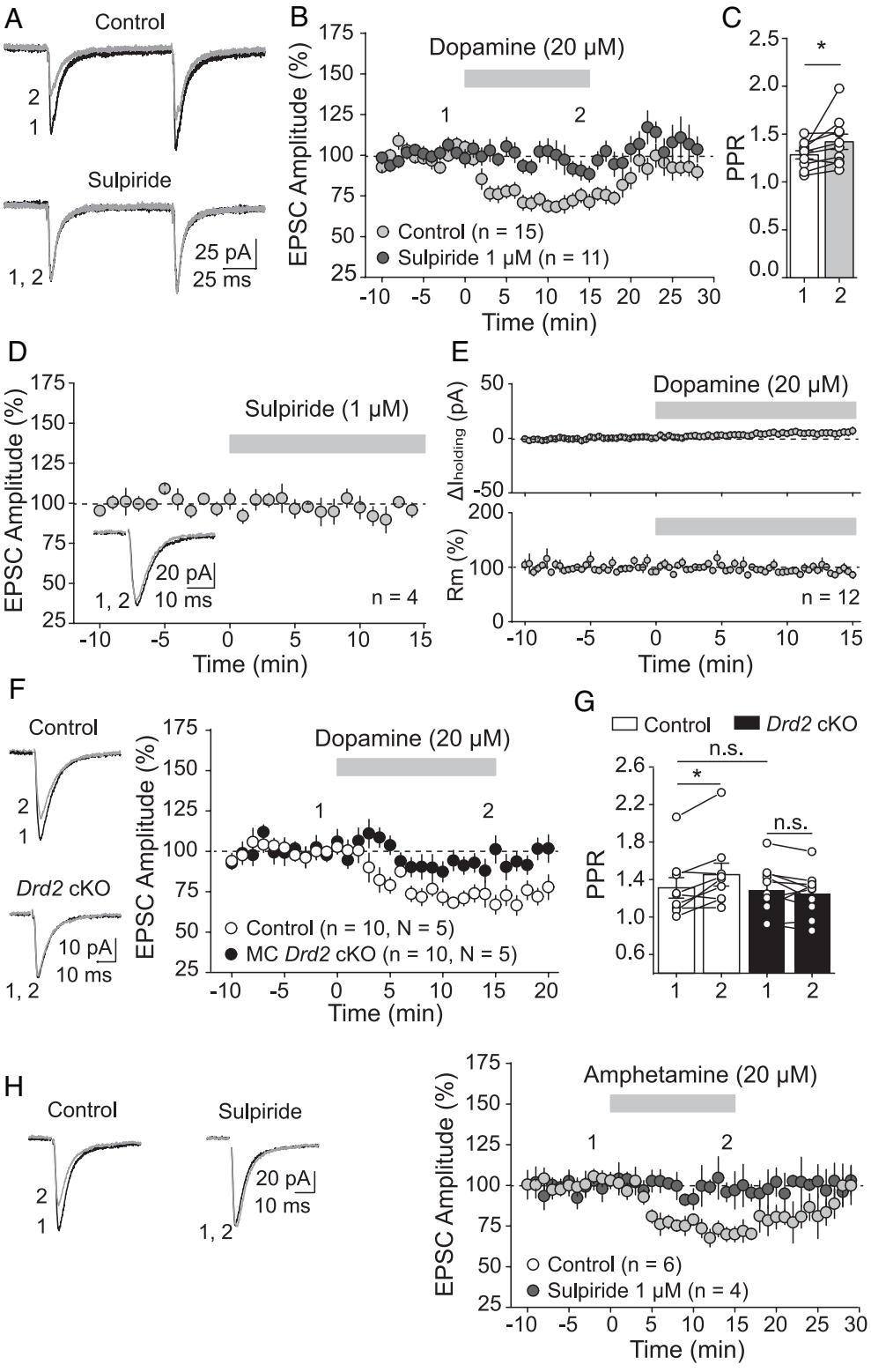

Fig. 6. Activation of MC D2Rs depressed MC-GC excitatory transmission. (*A–E*) Dopamine depressed MC-GC synaptic transmission in a D2-like receptor-dependent manner. (*A–C*) Representative average traces (*A*) and time-course summary plot (*B*) showing that bath application of dopamine (20 μM, 15 min) reduced MC-GC transmission in a reversible manner in control wild-type animals (Control: 71.3 ± 3.4% of baseline, n = 15, $P < 0.0001$, paired *t* test). This reduction was blocked in the continuous presence of the D2-like receptor antagonist sulpiride (1 μM) (sulpiride: 93.5 ± 5.9% of baseline, n = 11, $P = 0.1$, paired Wilcoxon signed ranks test; control vs. sulpiride: $P = 0.0009$, Mann–Whitney *U* test). The reduction was also associated with significant increase in PPR (*C*, pre: 1.28 ± 0.43, dopamine: 1.42 ± 0.08, n = 6, pre vs. dopamine: $P = 0.048$, paired *t* test). (*D*) Representative average traces and time-course summary plot showing that bath application of sulpiride (1 μM, 15 min) did not significantly affect MC-GC EPSC amplitude (95.0 ± 5.0% of baseline, n = 4, $P = 0.34$, paired *t* test). (*E*) No significant changes in GC holding current ($\Delta I_{holding}$, *Top*: 5.4 ± 3.2 pA difference from baseline, n = 12, $P = 0.19$, paired *t* test) or GC membrane resistance (Rm, *Bottom*: 96.5 ± 5.2% of baseline, n = 12, $P = 0.60$, paired *t* test) were observed during dopamine application in *B*. (*F* and *G*) Dopamine depresses MC-GC transmission via MC D2Rs. (*F*) Representative average traces (*Left*) and time-course summary plot (*Right*) showing that dopamine-mediated depression of MC-GC transmission was abolished in MC *Drd2* cKO animals as compared to Control mice (Control: 70.7 ± 4.1% of baseline, n = 10, $P = 0.00025$, paired *t* test; cKO: 93.5 ± 4.3% of baseline, n = 10, $P = 0.41$, paired Wilcoxon signed-rank test; control vs. cKO: $P = 0.0007$, Mann–Whitney *U* test). (*G*) Dopamine application significantly increased PPR in Control mice (pre: 1.31 ± 0.11, dopamine: 1.45 ± 0.12, n = 9, pre vs. dopamine: $P = 0.039$, paired Wilcoxon signed rank test), but not in MC *Drd2* cKO (pre: 1.29 ± 0.08, dopamine: 1.25 ± 0.07, n = 10, pre vs. dopamine: $P = 0.70$, paired *t* test). Basal PPR was similar in Control and MC *Drd2* cKO animals (Control: 1.31 ± 0.11%, n = 9; cKO: 1.29 ± 0.08%, n = 10; Control vs. cKO: $P = 0.97$, Mann–Whitney *U* test). (*H*) Amphetamine depressed MC-GC transmission in a D2-like receptor-dependent manner. Representative average traces (*Left*) and summary plot (*Right*) showing that bath applying D-amphetamine hemisulphate (20 μM, 15 min) reversibly depressed MC-GC synaptic transmission in control (70.8 ± 2.9% of baseline, n = 6, $P = 0.0019$, paired *t* test) but not in the continuous presence of sulpiride (1 μM) (sulpiride: 99.2 ± 8.7% of baseline, n = 4, $P = 0.99$, paired *t* test; control vs. sulpiride, $P = 0.041$, unpaired *t* test). Data are represented as mean ± SEM. *$P < 0.05$, n.s. $P > 0.3$.

It is well established that hippocampal dopaminergic signaling is required for hippocampus-dependent learning and memory (46). Novel events trigger dopamine release to the hippocampus (23, 24), and pharmacologic and knockout studies support a role for both hippocampal D1-like and D2-like receptors in both spatial and ORM (46, 47). We gathered functional and anatomical evidence supporting the argument that MC D2Rs negatively regulate the excitatory output of MCs onto GCs via a presynaptic mechanism. Previous autoradiography work suggested that D2Rs are expressed in MC axons while absent from GCs in cats and humans (18). Presumably due to the low specificity and sensitivity of D2R antibodies, several studies have inferred the expression of dopamine receptors from mRNA analysis (17). In the DG, the expression of a reporter from the *Drd2* promoter occurred in MCs but not GCs and INs (15, 16). Taking advantage of the SEP-tagged D2R KI mice (43, 44), we found enriched D2R expression in putative MC axons. In contrast, we did not detect D2Rs in MC somatodendritic compartment. As the live labeling approach only

detects SEP molecules residing outside of the plasma membrane (via the N-terminal localization on D2Rs) it is highly unlikely that SEP puncta represent membrane-bound SEP molecules that are not fused to D2R. However, we examined the potential of ectopic expression of SEP-D2Rs in the IML by colabeling with VGlut1 and VGAT, and as predicted by the reporter experiments, SEP-D2R expression was exclusive to VGlut1 (+) terminal structures—i.e., putative MC axon boutons. This was our first application of the SEP-D2R knocking mouse to visualize hippocampal dopamine receptor localization. The activity-dependent regulation of IML D2Rs remains to be characterized, though our data suggest that the SEP-D2R knockin mouse is a suitable model for such studies. Our functional analyses using the endogenous ligand dopamine did not detect any D2R-dependent modulation of MC active or passive membrane properties (*SI Appendix*, Fig. S4). Intriguingly, a previous study reported that the D2-like agonist quinpirole increases MC excitability (22), but whether a selective D2R antagonist can block this effect is unclear. While our results discarded that D2Rs regulate MC functional properties and excitatory inputs onto MCs (*SI Appendix*, Fig. S3), we cannot exclude additional effects at MC-INs synapses. However, the proconvulsant effect observed in MC *Drd2* cKO mice (Fig. 4) suggests that MC D2R signaling has a net inhibitory role in the DG.

Consistent with a presynaptic localization of D2Rs, we found that their activation with dopamine triggered a significant and reversible reduction in MC-GC transmission, which was associated with PPR increase and abolished by D2-like antagonism and *Drd2* deletion from MCs. The D2R-mediated suppression of glutamate release is likely due to the $G_{i/o}$-mediated inhibition of presynaptic calcium influx via voltage-gated calcium channels and/or activation of potassium channels (17). In addition, the psychostimulant amphetamine, known to potently promote the release of dopamine, also mediated a reversible D2R-dependent depression of MC-GC synaptic transmission. A previous study reported that transient bath application of dopamine and amphetamine induced a D2R-dependent, presynaptic long-term depression at neighboring perforant path inputs onto GCs (48). While the mechanism by which D2R activation induces this plasticity remains unclear, distinct D2R downstream signaling could account for the different durations of the D2R-mediated depression across synapses.

MC-GC excitatory transmission can powerfully activate GCs throughout the DG (49). We have recently reported that retrograde endocannabinoid signaling strongly suppresses glutamate release from MC axon terminals by activating presynaptic Type 1 cannabinoid receptors, another $G_{i/o}$-coupled receptor highly expressed in MC axon boutons (50). Endocannabinoid signaling is typically induced by GC activity, thereby suppressing MC inputs onto active GCs only. In contrast, the extensive dopaminergic projection throughout the hippocampus (3, 24) strongly suggests that dopamine effectively inhibits MC excitatory drive onto GCs by diffusely targeting MC D2Rs. Thus, dopaminergic and endocannabinoid signaling may have distinct but complementary ways of controlling MC-GC synaptic transmission and DG network activity. Such synergism mediated by different presynaptic $G_{i/o}$-coupled receptors likely represents a general motif throughout the brain that regulates neuronal communication and behavior (51).

Deleting *Drd2* from hilar MCs selectively impaired OLM but not ORM. These findings are consistent with recent studies implicating MCs in spatial memory (5–7). For instance, optogenetic inhibition of MCs impaired OLM but not ORM (5). Similarly, inhibiting MCs by overexpressing Kir2.1 potassium channels interfered with spatial memory retrieval but did not affect ORM (6). It is well-established that hippocampus-dependent learning and memory require normal hippocampal dopaminergic signaling (46). Pharmacological and germline knockout studies support a role for hippocampal D2-like receptors in both spatial and ORM (46, 47). However, our study is unique in that it directly addresses the cell-specific function of MC D2Rs in DG-dependent behaviors. The DG plays a critical role in spatial memory discrimination (52–54), a computational process that minimalize the overlap between similar neural representations, thereby reducing memory interference. GC sparse activity, which is classically attributed to their unique intrinsic properties and their particularly strong inhibition, is believed to be critical for spatial pattern separation (55). Remarkably, exposure to novel objects triggers dopamine release in the hippocampus (23, 24). By reducing MC excitatory drive onto GC (Fig. 6), MC D2Rs engaged during the OLM could improve signal to noise and enable memory discrimination.

Our findings supporting an anxiolytic function of MC D2Rs are consistent with previous pharmacological studies reporting that D2R signaling can have anxiolytic effects in vivo and suggest that D2Rs on MCs significantly contribute to this effect. For instance, D2R agonists subcutaneously administered decreased mouse open-field thigmotaxis (40) and reduced rat ultrasonic vocalizations (56). Our data also provide a potential mechanism for the role of MCs in anxiety-like behaviors. Three independent studies reported that MC activity is anxiolytic in the EPM (8–10), although others did not observe this action (5, 6). Chemogenetic and optogenetic activation of MCs increased mouse open-arm time (8, 10), and specific removal of MCs by diphtheria toxin reduced mouse open-arm time in the EPM (9). The MC-mediated anxiolytic effect is likely due to increased inhibition of GCs (8, 10), consistent with the idea that a decrease in GC activity is associated with reduced levels of anxiety (9, 57, 58). We report that deleting D2Rs from MCs was anxiogenic presumably by removing the D2R-mediated inhibition of the MC excitatory drive on GCs, which results in less GC activity. Thus, our results not only align with previous observations indicating that a reduction in GC activity is anxiolytic but also uncover a physiological mechanism by which D2R signaling dampens anxiety during exploratory behaviors. Such a mechanism is likely to occur during exposure to novel environments, which reportedly triggers dopamine release (23, 24).

Anxiety tests often involve a spatial component, so lack of orientation might yield equal preference for anxiogenic and nonanxiogenic environments. MC *Drd2* cKO mice do not have equal preference for the open and closed arms of the EPM but rather spend ~80% of their time in the closed arms (Fig. 3). Similarly, they spent ~90% of their time at the edges of the open field. The behavior of MC *Drd2* cKO mice in the EPM (Fig. 3) and in response to kainic acid (Fig. 4) suggest an anxiolytic and net inhibitory role of MC D2Rs in the DG. It is worth noting that anxiety can interfere with animals' exploration of novel objects or environments, which is critical for memory task performance (1). However, we observed no significant difference in total exploration time between objects when comparing MC *Drd2* cKO vs. control animals. The spatial memory deficit and anxiety-like behavior observed in MC *Drd2* cKO mice likely reflect a state of disordered DG information processing, possibly related to the decision of approach and avoidance, which has been proposed previously to underlie both phenotypes (1, 4).

Recent studies showed that chemogenetic inhibition of MCs reduces experimentally induced seizures by kainic acid and pilocarpine (11, 12). Further, MC-GC synapses are robustly strengthened following initial seizures, whereas reducing MC-GC transmission reduces seizure activity (11, 12, 59). Our findings

demonstrating that MC D2Rs depress MC-GC transmission and play an anticonvulsant role are consistent with these findings. However, in the chronic mouse model of temporal lobe epilepsy, activation of surviving MCs is antiepileptic (5, 60), suggesting that the function of MC D2Rs may also differ significantly with the disease stage. There is good evidence that D2Rs play an antiepileptic role (27). For example, germline D2R knockout animals have a substantially higher seizure score than wild-type animals (28). In addition, D2R antagonists used as antipsychotics promote seizures in epileptic and nonepileptic patients, and antiparkinsonian treatments that stimulate D2Rs are antiepileptic (27). D2R expression is reduced in the temporal lobe of epileptic patients and in rodent models of temporal lobe epilepsy (27). Given the diffuse nature of dopamine release and extensive dopaminergic projections in the hippocampus (3, 24), signaling through MC D2Rs may be a mechanistic explanation for the antiepileptic role of D2Rs. Moreover, by dampening MC-GC transmission, MC D2Rs emerge as a potential target to dampen seizure activity. Although we cannot discard that potential rearrangements of the DG circuit in our MC *Drd2* cKO model could contribute to the behavioral and seizure phenotypes, most evidence supports that these phenotypes critically rely on D2R-dependent changes in MC-GC synaptic transmission.

In conclusion, our study supports that MC D2Rs serve an inhibitory role that facilitates information processing in the DG, spatial memory task performance, and normal exploration of anxiogenic environments. In addition, MC D2Rs likely prevent DG runaway activity that occurs during epileptic seizures, and they may also be implicated in schizophrenia and cognitive and mood disorders. Finally, strong D2R expression in the IML is conserved across species perhaps as a testament to the importance of MC D2Rs in hippocampal function including in humans. Tools to selectively activate MC D2Rs in vivo will be required to demonstrate the therapeutic potential of these receptors.

Materials and Methods

Drd2$^{fl/fl}$ (B6.129S4(FVB)-Drd2tm1.1Mrub/J, Strain #: 020631; The Jackson Laboratory), C57BL/6 (C57BL/6NCrl, Strain Code: 027; Charles River Laboratories), and SEP-D2R knockin mice (B6;129S7-*Drd2*$^{tm1.1Jtw}$/J, Strain #: 030537; The Jackson Laboratory) were used in this study. All animals were group housed in a standard 12:12 h light:dark cycle and had free access to food and water. Animals were bred, cared for, handled, and used according to protocols approved by the Institutional Animal Care and Use Committee at Albert Einstein College of Medicine and the Vollum Institute (Oregon Health & Science University), in accordance with guidelines from the NIH. Experimental procedures for MC *Drd2* conditional KO generation, confirmation of AAV expression and immunolabeling, examination of *Drd2* mRNA expression by RT-qPCR, behavioral testing (OF, ORM, OLM, and EPM), seizure induction and monitoring, visualization of hippocampal D2Rs using SEP-D2 knockin mice, acute hippocampal slice preparation, electrophysiology, and biocytin visualization for post hoc confirmation of MC identity are detailed in *SI Appendix, Supplementary Materials and Methods*. Details of image acquisition and quantification, and of all statistical analyses performed are also included in *SI Appendix, Supplementary Materials and Methods*. For all additional details, refer to *SI Appendix, Supplementary Materials and Methods*.

Data, Materials, and Software Availability. This study did not generate new unique reagents. All raw data corresponding to main and supplemental figures are deposited in an online database: https://doi.org/10.25833/4g0f-bv50 (61). All other data are included in the manuscript and/or *SI Appendix*.

ACKNOWLEDGMENTS. We thank all members of the Castillo lab, especially Coralie Berthoux, for constructive feedback. We thank Maria Gulinello, director of the Albert Einstein College of Medicine Animal Behavior Core, for training and supervision of animal behavior experiments, Aubrey Siebels for assistance with the analysis of MC spontaneous activity, and Subrina Persaud for assistance with immunostaining, imaging, and brain and tissue processing in early stages of this project. We also thank Miwako Yamasaki (Hokkaido University) and Teresa A. Milner (Weill Cornell Medicine) for their attempt to detect D2Rs in the hippocampus using immunohistochemistry and immunoelectron microscopy, respectively. Finally, special thanks to John T. Williams (Vollum Institute, OHSU) for permitting Joseph J. Lebowitz to perform the experiments using SEP-D2R knockin mice. This research was supported by the NIH, R01-NS113600, R01-MH125772; R01-NS115543, and R01-MH116673 to P.E.C.; F31-MH122134 to M.C.G.; and F31-MH127810 to C.R. M.C.G. was partially supported by T32-GM007288; J.J.L. was supported by R01-DA004523 and T32-DA007262 grants; and D.-W.H. was supported by R01-NS083085. Confocal images were obtained at the Einstein Imaging Core (supported by the Rose F Kennedy Intellectual Disabilities Research Center–shared instrument grant NIH 1S10OD25295 to Konstantin Dobrenis). We thank Corwin Butler and Eric Schnell (Oregon Health and Science University and Portland Veterans Affairs Healthcare system) for assistance with antibodies for SEP-D2R labeling experiments. We acknowledge expert technical assistance by staff in the Advanced Light Microscopy Core in the Department of Neurology and Jungers Center at Oregon Health and Science University.

Author affiliations: [a]Dominick P. Purpura Department of Neuroscience, Albert Einstein College of Medicine, Bronx, NY 10461; [b]Vollum Institute, Oregon Health and Science University, Portland, OR 97239; [c]Department of Cell Biology, Albert Einstein College of Medicine, Bronx, NY 10461; and [d]Department of Psychiatry and Behavioral Sciences, Albert Einstein College of Medicine, Bronx, NY 10461

1. D. M. Bannerman *et al.*, Hippocampal synaptic plasticity, spatial memory and anxiety. *Nat. Rev. Neurosci.* **15**, 181–192 (2014).
2. T. Hainmueller, M. Bartos, Dentate gyrus circuits for encoding, retrieval and discrimination of episodic memories. *Nat. Rev. Neurosci.* **21**, 153–168 (2020).
3. B. A. Strange, M. P. Witter, E. S. Lein, E. I. Moser, Functional organization of the hippocampal longitudinal axis. *Nat. Rev. Neurosci.* **15**, 655–669 (2014).
4. H. E. Scharfman, The enigmatic mossy cell of the dentate gyrus. *Nat. Rev. Neurosci.* **17**, 562–575 (2016).
5. A. D. Bui *et al.*, Dentate gyrus mossy cells control spontaneous convulsive seizures and spatial memory. *Science* **359**, 787–790 (2018)
6. X. Li *et al.*, A circuit of mossy cells controls the efficacy of memory retrieval by Gria2I inhibition of Gria2. *Cell Rep.* **34**, 108741 (2021).
7. S. Li *et al.*, Alzheimer-like tau accumulation in dentate gyrus mossy cells induces spatial cognitive deficits by disrupting multiple memory-related signaling and inhibiting local neural circuit. *Aging Cell* **21**, e13600 (2022).
8. J. J. Botterill *et al.*, Bidirectional regulation of cognitive and anxiety-like behaviors by dentate gyrus mossy cells in male and female mice. *J. Neurosci.* **41**, 2475–2495 (2021).
9. S. Jinde *et al.*, Hilar mossy cell degeneration causes transient dentate granule cell hyperexcitability and impaired pattern separation. *Neuron* **76**, 1189–1200 (2012).
10. K. Y. Wang *et al.*, Elevation of hilar mossy cell activity suppresses hippocampal excitability and avoidance behavior. *Cell Rep.* **36**, 109702 (2021).
11. J. J. Botterill *et al.*, An excitatory and epileptogenic effect of dentate gyrus mossy cells in a mouse model of epilepsy. *Cell Rep.* **29**, 2875–2889.e6 (2019).
12. K. Nasrallah *et al.*, Seizure-induced strengthening of a recurrent excitatory circuit in the dentate gyrus is proconvulsant. *Proc. Natl. Acad. Sci. U.S.A.* **119**, e2201151119 (2022).
13. P. S. Buckmaster, H. J. Wenzel, D. D. Kunkel, P. A. Schwartzkroin, Axon arbors and synaptic connections of hippocampal mossy cells in the rat in vivo. *J. Comp. Neurol.* **366**, 271–292 (1996).
14. D. G. Amaral, H. E. Scharfman, P. Lavenex, The dentate gyrus: Fundamental neuroanatomical organization (dentate gyrus for dummies). *Prog. Brain Res.* **163**, 3–22 (2007).
15. G. Gangarossa *et al.*, Characterization of dopamine D1 and D2 receptor-expressing neurons in the mouse hippocampus. *Hippocampus* **22**, 2199–2207 (2012).
16. E. Puighermanal *et al.*, drd2-cre:ribotag mouse line unravels the possible diversity of dopamine d2 receptor-expressing cells of the dorsal mouse hippocampus. *Hippocampus* **25**, 858–875 (2015).
17. C. Missale, S. R. Nash, S. W. Robinson, M. Jaber, M. G. Caron, Dopamine receptors: From structure to function. *Physiol. Rev.* **78**, 189–225 (1998).
18. S. K. Goldsmith, J. N. Joyce, Dopamine D2 receptor expression in hippocampus and parahippocampal cortex of rat, cat, and human in relation to tyrosine hydroxylase–immunoreactive fibers. *Hippocampus* **4**, 354–373 (1994).
19. Y. Senzai, G. Buzsaki, Physiological properties and behavioral correlates of hippocampal granule cells and mossy cells. *Neuron* **93**, 691–704.e5 (2017).
20. D. Jung *et al.*, Dentate granule and mossy cells exhibit distinct spatiotemporal responses to local change in a one-dimensional landscape of visual-tactile cues. *Sci. Rep.* **9**, 9545 (2019).
21. J. J. Botterill, K. J. Gerencer, K. Y. Vinod, D. Alcantara-Gonzalez, H. E. Scharfman, Dorsal and ventral mossy cells differ in their axonal projections throughout the dentate gyrus of the mouse hippocampus. *Hippocampus* **31**, 522–539 (2021).
22. G. Etter, W. Krezel, Dopamine D2 receptor controls hilar mossy cells excitability. *Hippocampus* **24**, 725–732 (2014).
23. C. G. McNamara, A. Tejero-Cantero, S. Trouche, N. Campo-Urriza, D. Dupret, Dopaminergic neurons promote hippocampal reactivation and spatial memory persistence. *Nat. Neurosci.* **17**, 1658–1660 (2014).

24. T. Takeuchi *et al.*, Locus coeruleus and dopaminergic consolidation of everyday memory. *Nature* **537**, 357–362 (2016).
25. M. Piri, E. Ayazi, M. R. Zarrindast, Involvement of the dorsal hippocampal dopamine D2 receptors in histamine-induced anxiogenic-like effects in mice. *Neurosci. Lett.* **550**, 139–144 (2013).
26. Y. Bozzi, D. Vallone, E. Borrelli, Neuroprotective role of dopamine against hippocampal cell death. *J. Neurosci.* **20**, 8643–8649 (2000).
27. Y. Bozzi, E. Borrelli, The role of dopamine signaling in epileptogenesis. *Front. Cell Neurosci.* **7**, 157 (2013).
28. M. Dunleavy, G. Provenzano, D. C. Henshall, Y. Bozzi, Kainic acid-induced seizures modulate Akt (SER473) phosphorylation in the hippocampus of dopamine D2 receptor knockout mice. *J. Mol. Neurosci.* **49**, 202–210 (2013).
29. A. Wilkerson, E. D. Levin, Ventral hippocampal dopamine D1 and D2 systems and spatial working memory in rats. *Neuroscience* **89**, 743–749 (1999).
30. K. Yang *et al.*, Dopamine receptor activity participates in hippocampal synaptic plasticity associated with novel object recognition. *Eur. J. Neurosci.* **45**, 138–146 (2017).
31. H. Du *et al.*, Dopaminergic inputs in the dentate gyrus direct the choice of memory encoding. *Proc. Natl. Acad. Sci. U.S.A.* **113**, E5501–E5510 (2016).
32. E. A. Petter *et al.*, Elucidating a locus coeruleus-dentate gyrus dopamine pathway for operant reinforcement. *Elife* **12**, e83600 (2023).
33. A. Sík, N. Hájos, A. Gulácsi, I. Mody, T. F. Freund, The absence of a major Ca2+ signaling pathway in GABAergic neurons of the hippocampus. *Proc. Natl. Acad. Sci. U.S.A.* **95**, 3245–3250 (1998).
34. J. E. Zachry *et al.*, Sex differences in dopamine release regulation in the striatum. *Neuropsychopharmacology* **46**, 491–499 (2021).
35. O. O. F. Williams, M. Coppolino, S. R. George, M. L. Perreault, Sex differences in dopamine receptors and relevance to neuropsychiatric disorders. *Brain Sci.* **11**, 1199 (2021).
36. A. Vogel-Ciernia, M. A. Wood, Examining object location and object recognition memory in mice. *Curr. Protoc. Neurosci.* **69**, 8.31.1–8.31.17 (2014).
37. N. J. Broadbent, L. R. Squire, R. E. Clark, Spatial memory, recognition memory, and the hippocampus. *Proc. Natl. Acad. Sci. U.S.A.* **101**, 14515–14520 (2004).
38. M. R. Hunsaker, J. S. Rosenberg, R. P. Kesner, The role of the dentate gyrus, CA3a, b, and CA3c for detecting spatial and environmental novelty. *Hippocampus* **18**, 1064–1073 (2008).
39. F. Fredes, R. Shigemoto, The role of hippocampal mossy cells in novelty detection. *Neurobiol. Learn. Mem.* **183**, 107486 (2021).
40. P. Simon, R. Dupuis, J. Costentin, Thigmotaxis as an index of anxiety in mice. Influence of dopaminergic transmissions. *Behav. Brain Res.* **61**, 59–64 (1994).
41. A. A. Walf, C. A. Frye, The use of the elevated plus maze as an assay of anxiety-related behavior in rodents. *Nat. Protoc.* **2**, 322–328 (2007).
42. M. Levesque, M. Avoli, The kainic acid model of temporal lobe epilepsy. *Neurosci. Biobehav. Rev.* **37**, 2887–2899 (2013).
43. B. G. Robinson *et al.*, Desensitized D2 autoreceptors are resistant to trafficking. *Sci. Rep.* **7**, 4379 (2017).
44. J. J. Lebowitz *et al.*, Subcellular localization of D2 receptors in the murine substantia nigra. *Brain Struct. Funct.* **227**, 925–941 (2022).
45. E. S. Calipari, M. J. Ferris, Amphetamine mechanisms and actions at the dopamine terminal revisited. *J. Neurosci.* **33**, 8923–8925 (2013).
46. T. Tsetsenis, J. I. Broussard, J. A. Dani, Dopaminergic regulation of hippocampal plasticity, learning, and memory. *Front. Behav. Neurosci.* **16**, 1092420 (2023).
47. J. Rocchetti *et al.*, Presynaptic D2 dopamine receptors control long-term depression expression and memory processes in the temporal hippocampus. *Biol. Psychiatry* **77**, 513–525 (2015).
48. Y. Mu, C. Zhao, F. H. Gage, Dopaminergic modulation of cortical inputs during maturation of adult-born dentate granule cells. *J. Neurosci.* **31**, 4113–4123 (2011).
49. Y. Hashimotodani *et al.*, LTP at hilar mossy cell-dentate granule cell synapses modulates dentate gyrus output by increasing excitation/inhibition balance. *Neuron* **95**, 928–943.e3 (2017).
50. K. R. Jensen, C. Berthoux, K. Nasrallah, P. E. Castillo, Multiple cannabinoid signaling cascades powerfully suppress recurrent excitation in the hippocampus. *Proc. Natl. Acad. Sci. U.S.A.* **118**, e2017590118 (2021).
51. D. M. Lovinger *et al.*, Local modulation by presynaptic receptors controls neuronal communication and behaviour. *Nat. Rev. Neurosci.* **23**, 191–203 (2022).
52. J. K. Leutgeb, S. Leutgeb, M. B. Moser, E. I. Moser, Pattern separation in the dentate gyrus and CA3 of the hippocampus. *Science* **315**, 961–966 (2007).
53. T. J. McHugh *et al.*, Dentate gyrus NMDA receptors mediate rapid pattern separation in the hippocampal network. *Science* **317**, 94–99 (2007).
54. A. Treves, E. T. Rolls, Computational analysis of the role of the hippocampus in memory. *Hippocampus* **4**, 374–391 (1994).
55. R. P. Kesner, E. T. Rolls, A computational theory of hippocampal function, and tests of the theory: New developments. *Neurosci. Biobehav. Rev.* **48**, 92–147 (2015).
56. G. D. Bartoszyk, Anxiolytic effects of dopamine receptor ligands: I. Involvement of dopamine autoreceptors. *Life Sci.* **62**, 649–663 (1998).
57. C. Anacker *et al.*, Hippocampal neurogenesis confers stress resilience by inhibiting the ventral dentate gyrus. *Nature* **559**, 98–102 (2018).
58. E. Engin *et al.*, Modulation of anxiety and fear via distinct intrahippocampal circuits. *Elife* **5**, e14120 (2016).
59. K. Nasrallah *et al.*, Retrograde adenosine/A2A receptor signaling mediates presynaptic hippocampal LTP and facilitates epileptic seizures. bioRxiv [Preprint] (2021). https://doi.org/10.1101/2021.10.07.463512 (Accessed 9 October 2021).
60. C. R. Butler, G. L. Westbrook, E. Schnell, Adaptive mossy cell circuit plasticity after status epilepticus. *J. Neurosci.* **42**, 3025–3036 (2022).
61. M. C. Gulfo *et al.*, Notebook Database for Dopamine D2 receptors in hilar mossy cells regulate excitatory transmission and hippocampal function. LabArchives. https://doi.org/10.25833/4g0f-bv50. Deposited 3 October 2023.